Lab on a Chip

Accepted Manuscript

ROYAL SOCIETY OF CHEMISTRY

www.rsc.org/loc

Dynamic Trapping and Two-Dimensional Transport of Swimming Microorganisms Using a Rotating Magnetic Micro-Robot

Zhou Ye and Metin Sitti*

Department of Mechanical Engineering, Carnegie Mellon University, Pittsburgh, Pennsylvania 15213, USA

* Corresponding author: sitti@cmu.edu

Keywords: Microfluidic trapping, dynamic transportation, micro-robot, swimming, microorganism

Abstract

Manipulation of microorganisms with intrinsic motility is a challenging yet important task for many biological and biomedical applications. Currently, such a task has only been accomplished using optical tweezers, while at the risk of averse heating and photodamage of the biological samples. Here we proposed a new micro-robotic approach for fluidic trapping and two-dimensional transportation of motile microorganisms near a solid surface in fluids. We demonstrated selective trapping and transportation of individual freely swimming multi-flagellated bacteria over a distance of 30 μm (10 bodylength of the particle) on a surface, using the rotational flows locally induced by a rotating magnetic micro-particle. Only a weak uniform magnetic field (< 3 mT) was applied to actuate the micro-particle. The micro-particle can translate on a glass substrate by rotation at a speed of up to 100 μm/s, while providing a fluidic force of a few to tens of pico-Newtons.

Introduction

Optical tweezers has been a common tool for trapping and manipulation of motile microorganisms such as flagellated bacteria[1-3]. Limitations of this technique include the possible photodamage induced by high intensity laser[4] and the cost and complexity of the optical setup[5]. Magnetic tweezers is a possible alternative, but requires additional magnetic labeling[6-8]. The other existing techniques, including dielectrophoresis[9-11], electrostatics[12], acoustic trapping[13], magnetic trapping[14] and microfluidics[15-17], provide static trapping possibilities, but their capability of selective trapping and manipulation of a swimming microorganism has not been demonstrated yet. On the other hand, recent developments in untethered mobile micro-robotics[18,19] have proven their use for precise and local manipulation of microspheres[20,21], non-motile living cells[22-24] and cell-laden micro-gels[25], but trapping and manipulation of microorganisms with swimming motility have not been achieved yet using such micro-robotic techniques.

Inspired by our previous work on micro-robotic microparticle manipulation[26], we propose a mobile micro-robotic approach to selectively trap and transport individual microorganisms swimming close to a planar surface at low Reynolds number ($Re < 10^{-2}$) without any contact using local rotational fluid flows induced by fast-rotating spherical Neodymium-Iron-Boron (NdFeB) micro-particles. A shear-induced force pointing toward the center of the rotational flow field provides the trapping force. Selective, non-contact trapping and transportation is made possible given the rapid decay of flow intensity from the center of the locally induced flow field. Adverse effects on swimming microorganisms are eliminated as only hydrodynamic forces are involved. A weak uniform magnetic field (< 3.5 mT) is applied to rotate the magnetic micro-particles. Moreover, no special surface or spatial pattern is necessary to perform the trapping and transportation, which enables a versatile approach.

Therefore, it is possible to incorporate the proposed approach with any existing microfluidic system directly. Finally, for swimming microorganism trapping and manipulation demonstrations, a highly motile (mean speed of around 26 μm/s) multi-flagellated bacteria[27,28], *Serratia marcescens*, are used as example swimming microorganisms.

Methods and Materials

Rotational-Flow-based Micro-Robotic Object Manipulation Method. When a spherical magnetic micro-particle rotates inside a viscous fluid near a solid surface with rotation axis perpendicular to the surface (termed as spinning), a rotational flow field is locally induced around the particle. At low *Re*, the rotational flows are circumferential with concentric streamlines centered on the rotation axis of the particle. A numerical simulation of a sphere spinning at 100 Hz, corresponding to a rotation speed of 6000 rpm, near a solid boundary in water has been carried out in COMSOL. The simulation result is given in Fig. 1a, which shows the circular streamlines of the induced flows and the rapid decay of flow velocity from the sphere. An object exposed in such rotational flow field would experience drag force exerted by the surrounding fluid, which acts to push the object to follow the streamline at the hydrodynamic center of the object. In addition, any object with geometric anisotropy will be oriented by the flow to minimize the viscous surface stress. For a motile microorganism such as a bacterium, it is minimally affected by the induced rotational flow when it is far from the rotating particle. However, when it is in the vicinity of the particle, it is possible that it can be re-oriented to align the long axis of its cell body as well as the flagella with the streamlines if the flows are strong enough so that the viscous drag overwhelms bacterium's propulsion from

flagella. After reorientation, the bacterium is trapped inside the rotational flow and orbits the rotating particle. Such process is depicted in Fig. 1b.

To enable dynamic position control of the locally induced flows for object transportation and manipulation, the actuation method reported in our previous work that takes advantage of the geometric isotropy of the spherical particle is adopted: Instead of keeping the rotation axis of the particle perpendicular to the surface, we tilt it by a small angle. Then the rotation can be decomposed into two orthogonal components: one perpendicular to the surface - ω_s, as previously introduced, to generate rotational flows, and the other parallel to the surface - ω_r, which turns particle's rotation into linear translation of its position on the surface via frictional forces. Therefore, the position of the induced rotational flows is instantly determined by controlling the translational motion of the particle in real-time, as described in Fig. 1c. By changing both the rotation frequency and the tilt angle, we can adjust the intensity of the induced rotational flows as well as the translational speed in a coupled manner. The flow fields induced by pure particle spinning ($\theta = 90^\circ$) will be changed by the flow fields introduced by the particle rolling and the resulting translational motion of the particle. Due to the linearity of low Reynolds-number flows, the flow field during transportation can be treated as a linear superposition of the flows induced by ω_s, ω_r, and the translational motion of the particle. At large tilt-angles, the spinning component is more dominant. For example, at $\theta = 75^\circ$, $\omega_r/\omega_s = \cos\theta/\sin\theta = 0.27$. Further, the translational speed resulting from ω_r, due to significant slippage, is much less than when there is no slippage, and hence the flows induced by such translational motion is far less significant than those induced by rotational motion of the particle, especially at high rotation speeds. To visualize the flow field during transportation, a simulation shown in Fig. 1d is carried out. The flows are majorly circulating

the rotating particle, while there exist out-of-plane velocity components arising from the rolling component of rotation. However, these components are relatively insignificant compared to the circulating flows especially at $r \approx 1.5a$, as shown by the normalized out-of-plane velocity components. Therefore, the flows induced by the spinning component dominate in the flow field, which enables stable trapping of microorganisms during translation.

Potential hydrodynamic damage by the induced rotational flows to microorganisms with cell walls, such as bacteria, is minimal due to the high tensile strength of the cell walls[29]. For cells without walls, such as animal cells, the potential damage needs to be investigated with care. The shear rate of the induced rotational flow can be approximated as[26]: $\gamma = -2.43\omega(a/r)^{3.43}$, where ω is the rotation speed, a is the radius of the magnetic particle, and r is the distance from the particle center. The maximum shear rate that occurs at $r = a$ for a spherical particle spinning at 110 Hz is estimated to be 1680 s^{-1}, and the corresponding shear stress in water would be 1.68 Pa. However, one should notice that the shear rate decreases exponentially with distance. For example, at $r = 1.5a$, where cells are more likely to stay in the dynamic trap, the shear rate and shear stress drop rapidly to 418 s^{-1} and 0.4 Pa, respectively. No damage to animal cells has been reported at such shear rate and stress values under laminar flow conditions[30]. In addition, the above shear stress estimation was made on a static object. In practice, the trapped cells always orbit around the rotating particle along with the induced flows, and thus the shear stress they experience would further diminish, making it even less possible for any damage to occur. Therefore, the proposed method is expected to cause no adverse effects on the targeted biological samples such as motile microorganisms.

Cell growth. *Serratia marcescens* (ATCC 274, American Type Culture Collection, Manassas, VA) was cultured to exponential growth phase in liquid nutrient broth (25 g Difco LB Miller Broth and 1 L deionized (DI) water, pH 7.0) by incubating on a shaker at 37°C for about 3.5 - 4 hours. The liquid culture was diluted 1:10 in motility medium (0.01 M KH_2PO_4, 0.067M NaCl, 10^{-4} M EDTA, 0.01M glucose, pH = 7.0) before experiments.

Sample preparation. Magnetic particles with a diameter of 4 ± 1 μm were obtained via filtering the spherical Neodymium-Iron-Boron powder (MQP-S-11-9-20001-070, Magnequench International, Inc.) through membrane filters with pore size 5 μm (K50CP04700, Osmonics, Inc.) and 3 μm (K30CP02500, Osmonics, Inc.) sequentially. The residues on the 3-μm membrane filter were then collected for bacteria trapping and transport experiments. The experiments were performed in a 5 mm x 5 mm x 2 mm chamber constructed from a polydimethylsiloxane square frame sandwiched between two glass coverslips. Magnetic particles were magnetized *in-situ* with a permanent magnet providing a magnetizing field of 1 T.

Magnetic coil system. Uniform rotating magnetic fields were generated using an electromagnetic coil system consisting of three sets of electromagnets for in-plane and out-of-plane fields respectively (see Supplementary Figure. S1). Two pairs of iron-cored electromagnets that were perpendicular to each other were used to generate in-plane fields, while the out-of-plane field was generated by a third vertically placed solenoid. The coil system was built onto a microscope stage insert so that it could be placed into an inverted microscope (Axio Observer, Carl Zeiss) rigidly. Currents through the coils were generated by

motor drivers (Syren 10, Dimension Engineering LLC) controlled with an Arduino Uno R3 microcontroller board to enable high frequency micro-particle rotation control. A desktop computer with customized user interface program communicated with the microcontroller to achieve real-time adjustment of magnetic field parameters. The magnetic field strength was calibrated using a gauss meter probe (Model 410, Lake Shore Cryotronics, Inc.). Magnetic fields up to 3.5 mT could be generated by the given coil system.

Results and Discussion

The proposed approach is experimentally verified by rotating an NdFeB micro-particle with 4-μm diameter at 110 Hz with a tilt angle of 75° from the surface in aquatic media using a uniform magnetic field of 2 mT. A diluted population of flagellated bacteria, *Serratia marcescens*, is added to the media. The experimental demonstration of transportation of the bacterium close to a glass substrate is shown in Fig. 2. When a freely swimming bacterium approaches the micro-particle resting on the surface, the rotational magnetic field is turned on to initiate rotation of the particle and hence the induced rotational flows (Fig. 2b). The bacterium is reoriented and trapped immediately if the intensity of the flow is large enough. The trapped bacterium is carried with the rotating particle as it translates on the surface in two-dimensions (2D) (Fig. 2c-e), and hence can be transported to any location in 2D precisely in the given workspace. To release the bacterium, the rotation of the particle is simply turned off and the bacterium can retrieve its original motility (Fig. 2f-h). During trapping and transportation, the trapped bacterium is observed to remain close to the rotating particle, with a distance less than 0.5 body-length of the particle. When released, the trapped bacterium could be expected to appear on any position within that distance. Therefore, the position

tolerance can be determined as 1 body-length from the particle center, which is 4 μm in this work. This could be improved by introducing feedback control to the current setup and automating the process[26] as a future work.

Successful trapping of motile microorganisms such as bacteria requires that the fluidic drag exerted on the cell body for reorientation dominates the microorganism's own propulsive force. A numerical simulation is thus carried out to examine the influences of various parameters on the fluidic force experienced by a flagellated bacterium. In the simulation, the bacterium's cell body is modeled as a 2-μm-in-length cylinder with a diameter of around 500 nm located near a 5-μm-in-diameter spinning sphere on a surface at a distance of 0.5 radius of the sphere to its center. The following parameters are tested, including rotation frequency of the spherical particle, initial orientation of the bacterium, swimming speed of the bacterium, and its vertical position in the induced rotational flows. The results are shown in Fig. 3. The propulsive force generated by bacteria's flagella is estimated to be about 0.57 pN[31], so a ten times larger fluidic force, which is about 5.7 pN, should be sufficient to reorient the cell body. To achieve such a force, a rotation frequency of 90 Hz is necessary when the bacterium is located on the equatorial plane of the rotating particle at a distance of one particle radius, with its body's long axis tangential to local streamlines.

The induced rotational flow field travels instantly with the rotating particle, and hence we have also characterized the translational speed of the rotating particle. Figure 4a shows the case when the particle's rotation axis is parallel to the surface, resulting in pure translation without the rotational flows for trapping. It has been observed that the particle’s translational speed increases almost linearly along with rotation frequency up to around 100 Hz, and then saturates. Such saturation may result from the increasing hydrodynamic friction and lift force,

but further investigation for the cause would be necessary and is a future work. The maximum translational speed can reach up to 100 μm/s, which significantly surpasses the reported swimming speed of flagellated bacteria at 15-30 μm/s. The relationship between translational speed and tilt angle is revealed in Fig. 4b. The measured data are fitted into a cosine function of $y = a_1\cos(\theta + a_2)$. The variables a_1 and a_2 are found to be 80.19 and -9.565, respectively, with an R-square value of 0.9739. At a tilt angle of 75°, the translational speed is maintained at 32 μm/s, which is about the same as the maximum swimming speed of bacteria. The equivalent spinning frequency for inducing the sufficient trapping rotational flows is 106 Hz with a full rotation frequency of 110 Hz.

Dynamic trapping implemented by the proposed method is different from that of the optical tweezers. Motile microorganisms trapped in the rotational flows will first realign their bodies to minimize the viscous stress applied from the surrounding flows, which reduces the chance for them to escape randomly from the flows. The trapping forces majorly arise from the shearing of the rotational flows, which is complicated in this case. A rough estimation of the forces has been discussed as[26] $F_t = Ca^2 v_{rel}|\gamma|^{0.5}$, where C is a constant determined by fluid properties and v_{rel} is the speed of the trapped microorganism relative to the surrounding flows. One should notice that γ is a nonlinear function of the radial position r of the trapped object, from which a relation between F_t and r can be obtained. However, considering the nonlinear nature of such relationship, a stiffness constant similar to that of the optical tweezers may not be easily achievable. An accurate analysis of the trapped force and the corresponding trapping stiffness requires further and detailed investigation on the complex hydrodynamics, which is a future work.

The proposed trapping method relies on low-*Re* ($Re \ll 1$) hydrodynamics. The proposed method is expected to be valid as long as $Re \ll 1$ is satisfied. Considering that *Re* is inversely proportional to the viscosity of fluid, any increase in the viscosity is in favor of the method as it further reduces *Re*. One possible downside of increasing viscosity is that actuating the magnetic micro-particle in a more viscous fluid requires higher magnetic torque input, which could limit the maximum rotation speed a micro-particle can reach.

Conclusions

Our proposed approach has shown the capability of dynamic trapping and 2D transportation of individual swimming microorganisms precisely without the necessity of any additional labeling on the biological samples or special surfaces or patterns. While such capability is also possible by using optical tweezers, our approach eliminates the risk of heating or photodamaging the biological samples, and is achievable using a much simpler and very versatile setup. While this study showed the rotational flow based local trapping and manipulation of *Serratia marcescens* bacteria, any swimming microorganism such as spermatozoids, bacteria and algae swimming close to a surface could be also trapped and transported in 2D selectively using the proposed method for possible future biological motile cell study and bioengineering applications. One possible future path for further development of our approach is to measure trapping forces exerted on individual motile microorganisms[32] by quantitative estimation of the hydrodynamic forces in the induced rotational flows.

References

1. Ashkin, A. & Dziedzic, J. M., Optical trapping and manipulation of viruses and bacteria. *Science* **235**, 1517-1520 (1987).

2. Grier, D., A revolution in optical manipulation. *Nature* **424**, 810-816 (2003).

3. Zhang, H. & Liu, K. K., Optical tweezers for single cells. *J. R. Soc. Interface* **5**, 671-690 (2008).

4. Mirsaidov, U. *et al*, Optimal optical trap for bacterial viability. *Phys.Rev. E* **78**, 021910 (2008).

5. Ranaweera, A., Investigations with optical tweezers: construction, identification, and control. *Doctoral Dissertation.* (2004).

6. Crick, F. & Hughes, A., The physical properties of cytoplasm: astudy by means of the magnetic particle method, Part II. Theoretical treatment. *Exp. Cell Res.* **1**(1), 37-80 (1950).

7. Wang, N., Butler, J. & Ingber, D., Mechanotransduction across the cell surface and through the cytoskeleton. *Science* **260**, 1124-1127 (1993).

8. Gosse, C. & Croquette, V., Magnetic tweezers: micromanipulation and force measurement at the molecular level. *Biophys. J.* **82**(6), 3314-3329 (2002).

9. Chiou, P. Y.; Ohta, A. T. & Wu, M. C., Massively parallel manipulation of single cells and microparticles using optical images. *Nature* 4**36**, 370-372 (2005).

10. Zhou, R., Wang, P. & Chang, H. C., Bacteria capture, concentration and detection by alternating current dielectrophoresis and self-assembly of dispersed single-wall carbon nanotubes. *Electrophoresis* **27**, 1376-1385 (2006).

11. Yang, L. *et al*, A multifunctional micro-fluidic system for dielectrophoretic concentration coupled with immuno-capture of low numbers of Listeria monocytogenes. *Lab Chip* **6**, 896-905 (2006).

12. Krishnan, M., Mojarad, N., Kukura, P. & Sandoghdar, V., Geometry-induced electrostatic trapping of nanometric objects in a fluid. *Nature* **467**, 692-695(2010).

13. Shi, J. *et al.*, Focusing microparticles in a microfluidic channel with standing surface acoustic waves (SSAW). *Lab Chip* **8**, 221-223 (2008).

14. Demirörs, A. *et al*, Colloidal assembly directed by virtual magnetic moulds. *Nature*, **503**, 99-103 (2013).

15. Kim, M. C. *et al*, Programmed trapping of individual bacteria using micrometre-size sieves. *Lab Chip* **11**, 1089-1095 (2011).

16. Guo, P. *et al*, Microfluidic capture and release of bacteria in a conical nanopore array. *Lab Chip* 1**2**, 558-561 (2012).

17. Karimi, A., Yazdi, S. and Ardekani, A. M., Hydrodynamic mechanisms of cell and particle trapping in microfluidics. *Biomicrofluidics* 7, 021501 (2013).

18 Diller, E. and Sitti, M., Micro-scale mobile robotics. *Foundations and Trends in Robotics* **2**(3), 143-259 (2013).

19 Sitti, M., Miniature devices: voyage of the microrobots. *Nature* **458**, 1121-1122 (2009).

20 Pawashe, C., Floyd, S., Diller, E. and Sitti, M., Two-dimensional autonomous micro-particle manipulation strategies for magnetic micro-robots in fluidic environments. *IEEE Trans. on Robotics* **28**(2), 467-477 (2012).

21 Floyd, S., Pawashe, C. and Sitti, M., Two-dimensional contact and noncontact micro-manipulation in liquid using an untethered mobile magnetic microrobot. *IEEE Trans. on Robotics* **25**(6), 1332-1342 (2009).

22. Steager, E. B. *et al*, Automated biomanipulation of single cells using magnetic microrobots. *Intl. J. Robot. Res.* **32**(3), 346-359 (2013).

23. Petit, T. *et al*, Selective trapping and manipulation of microscale objects using mobile microvortices. *Nano Lett.* **12**, 15-160 (2012).

24. Hu, W., Fan, Q. and Ohta, A. T., An opto-thermocapillary cell micromanipulator. *Lab Chip* **13**, 2285-2291 (2013).

25 Tasoglu, S., Diller, E., Guven, S., Sitti, M. and Demirci, U., Untethered micro-robotic coding of three-dimensional material composition. *Nature Comm.* **5**, DOI: 10.1038/ncomms4124 (2014).

26. Ye, Z., Diller, E. & Sitti, M., Micro-manipulation using rotational fluid flows induced by remote magnetic micro-manipulators. *J. Appl. Phys.* **112**, 064912 (2012).

27 Edwards, M. R., Carlsen, R. W., Zhuang, J. and Sitti, M., Swimming motility characterization of Serratia marcescens. *J. Micro-Bio Robotics*, in press.

28 Edwards, M. R., Carlsen, R. W. and Sitti, M., Three dimensional motion analysis of bacteria-driven microbeads near and away from walls. *Appl. Phys. Lett.* **102**(14), 143701 (2013).

29. Carpita, N., Tensile strength of cell walls of living cells. *Plant Physiol.* **79**, 485-588

(1985).

30. Chisti, Y., Hydrodynamic damage to animal cells. *Crit. Rev. Biotechnol.* **21**(2), 67–110 (2001)

31. Chattopadhyay, S., Moldovan, R., Yeung, C. & Wu, X. L., Swimming efficiency of bacterium *Escherichia coli*. *Proc. Natl. Acad. Sci.* **103**(37), 13712-13717 (2006).

32. Neuman, K. C. & Nagy, A., Single-molecule force spectroscopy: optical tweezers, magnetic tweezers and atomic force microscopy. *Nature Meth.* **5**, 491-505 (2008).

Supplementary Information is available in the online version of the paper.

Acknowledgements. We thank R. Wright Carlsen and J. Zhuang for their assistance with bacteria culturing, and E. Diller for his discussions. M.S. was funded by the National Science Foundation (NSF) Cyberphysical Systems Program (CNS-1135850) and the NSF National Robotics Initiative Program (NRI-1317477).

List of Figure Captions:

Figure 1. **Induced rotational flow fields by rotation of the magnetic micro-particle.** (a) Simulation result of a 5-μm diameter spherical micro-particle spinning at 100 Hz on a flat surface in water. The plot is from a top-view of the cross-section taken at the equatorial plane of the micro-particle. Red concentric circles represent the streamlines. Color map shows the flow velocity distribution. (b) Schematic of the trapping of a nearby bacterium by the rotational flow induced by the rotation ω of the spherical micro-particle near a flat surface. Any bacterium that is far away is minimally affected by the induced flow. A bacterium that is close enough to the spinning particle is first reoriented by the flow to align its body's long axis with the local streamline (i), and then get trapped (ii) and orbits around the particle. (c) Schematic of mechanism for enabling the mobility of induced rotational flow field. Instead of being perpendicular to the surface as shown in (b), the rotation axis of the particle is tilted from z-axis. If the tilt angle is defined as θ, then the original rotation can be decomposed into two components: $\omega_s = \omega \sin\theta$ to generate rotational flows for bacteria trapping, and $\omega_r = \omega \cos\theta$ to cause translation of the particle with a mean speed of v and carry along the bacteria with it due to the induced rotational flows on the surface. (d) Simulation result of a 5-μm diameter spherical micro-particle rotating at 100 Hz with a tilt-angle of $\theta = 75^\circ$ and a translational speed of $0.06\omega_r a$ in $-y$ direction on a flat surface in water. The plot is from a top-view of the cross-section taken at the equatorial plane of the micro-particle. The arrows indicate the in-plane flow velocity at selective positions, while the color map shows the distribution of out-of-plane flow velocity normalized by the magnitude of in-plane flow velocity at the same position.

Figure 2. **Trapping and transportation of living motile bacterium.** A 2 mT magnetic field was applied to rotate a 4-μm-in-diameter magnetic micro-particle with $\theta = 75^{\circ}$. The largest dark circle indicates the instant positions of the particle at given snapshots, while the small dot with a halo in the yellow circle shows the instant positions of the bacterium being manipulated. The bacterium was trapped and transported over a distance of 50 μm (12.5 bodylength of the particle) across the view.

Figure 3. **Microfluidic force on a bacterium's cell body.** Numerical simulations were performed to examine influences of various parameters on the microfluidic forces experienced by a bacterium cell body due to the induced rotational flows. The rotating magnetic micro-particle was modeled as a sphere spinning at 100 Hz on a flat surface, and the bacterium cell body was modeled as a 2 μm long cylinder with a 500 nm diameter. In each simulation, only one parameter was varied while others were all kept constant. (a) The microfluidic force increased linearly with the rotation frequency of the particle. For successful trapping, a fluidic force of $\geqslant$5.7pN was computed to be necessary, which corresponds to a rotation frequency of at least around 90 Hz. (b) The fluidic force decreases linearly with the relative velocity of the cell body to the background rotational flows. A negative sign of body velocity indicates that the body velocity is in the opposite direction of the background flow. (c) The fluidic force reached it maximum when the long axis of the cell body was perpendicular to the direction of the background flows ($\pm 90^{\circ}$), and was at its was minimum when the long axis was align with the background flows (0°). (d) The fluidic force reached its maximum when the cell body was on the equatorial plane of the spinning particle. The force decreased significantly as the cell

body deviated vertically from that plane. On the surface, the cell body only experienced a fluidic force that was 1/3rd of its maximum value.

Figure 4. **Translational speed of the rotating micro-particle.** A magnetic micro-particle of 4-μm diameter was used in experiments. (a) $\theta = 0^{\circ}$, only translational motion without inducing the rotational flows for trapping. In this case, the translational speed increased almost linearly with the rotation frequency up to 100 Hz, and then saturated. (b) Rotation frequency was kept at 110 Hz, while θ varied. Translational speed decreased as θ increased. Error-bars show the standard deviation of measurements over three sets of data.

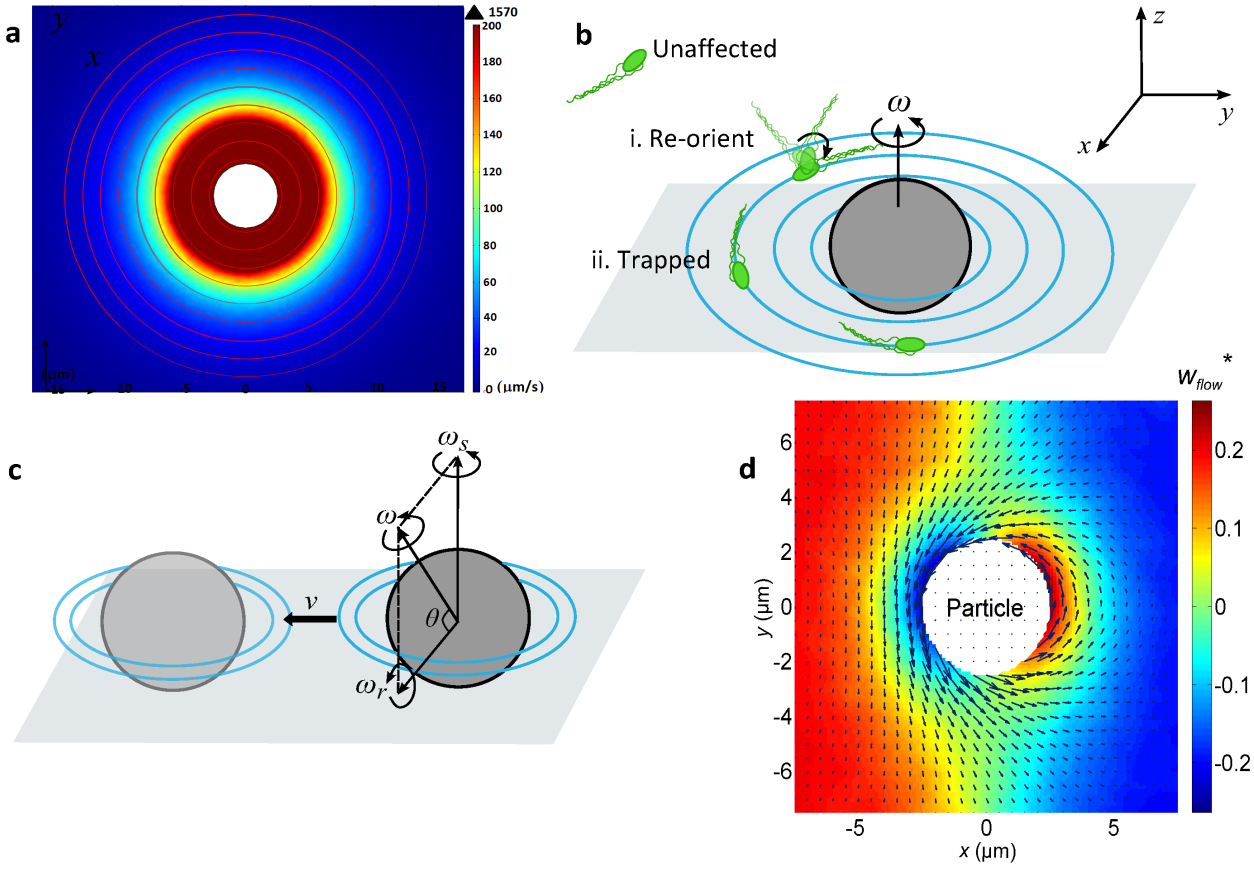

Figure 1

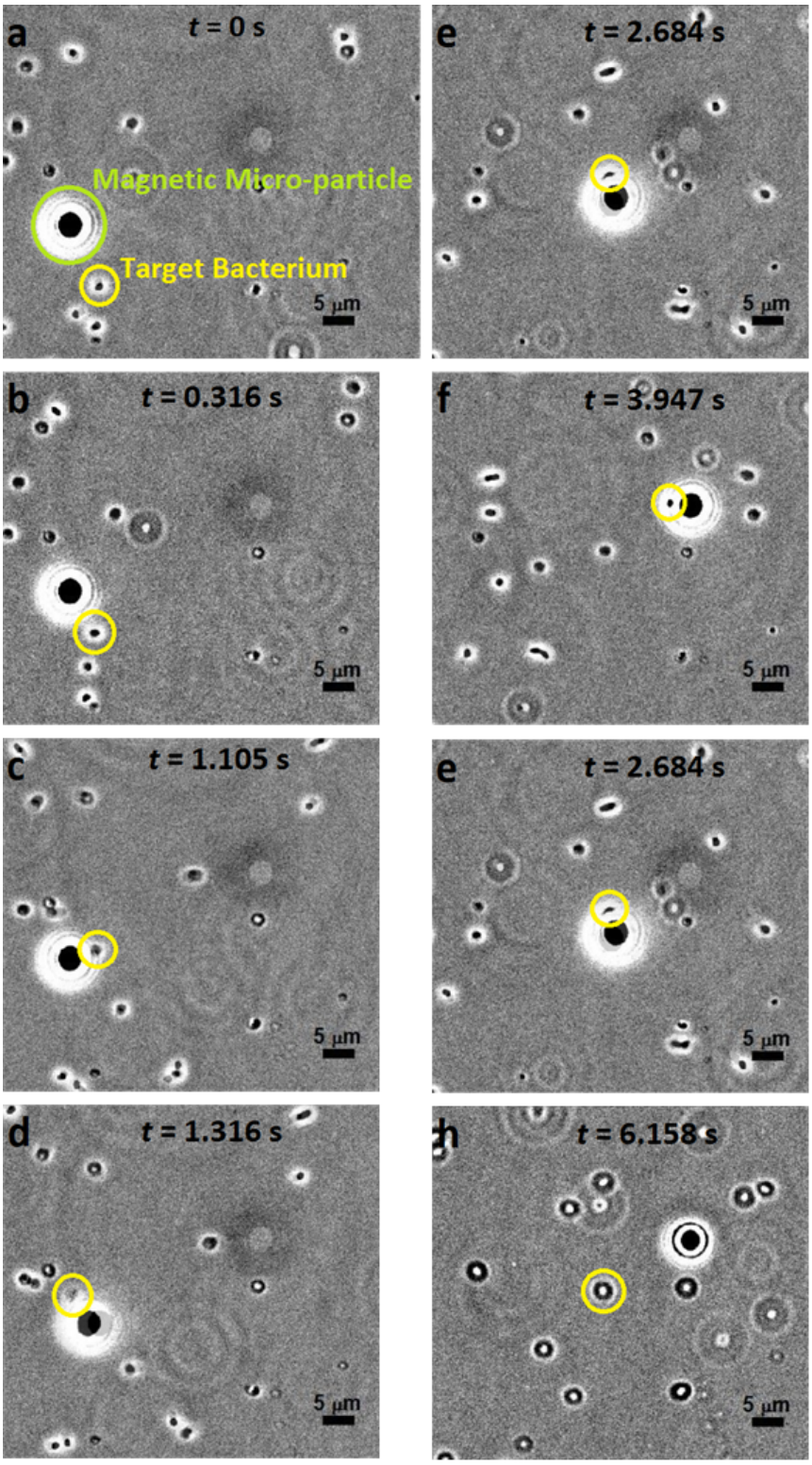

Figure 2

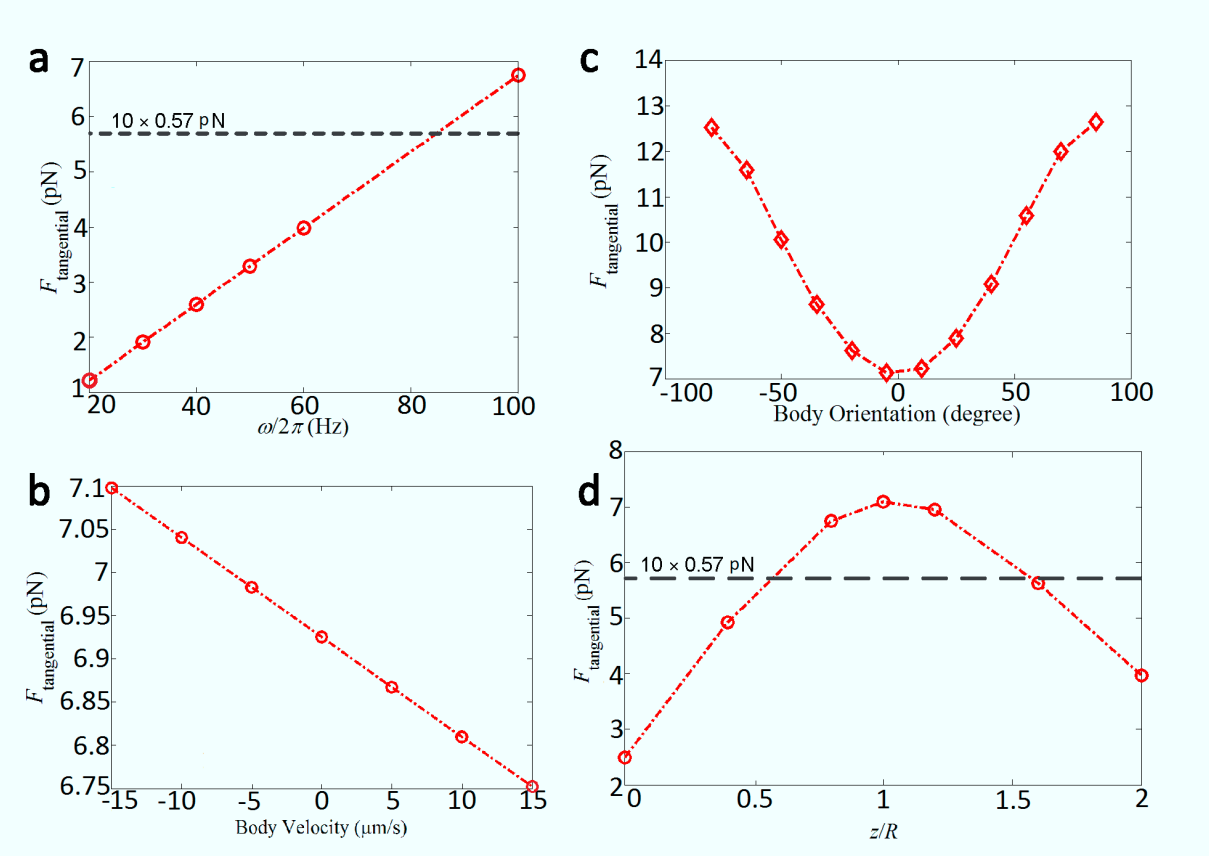

Figure 3

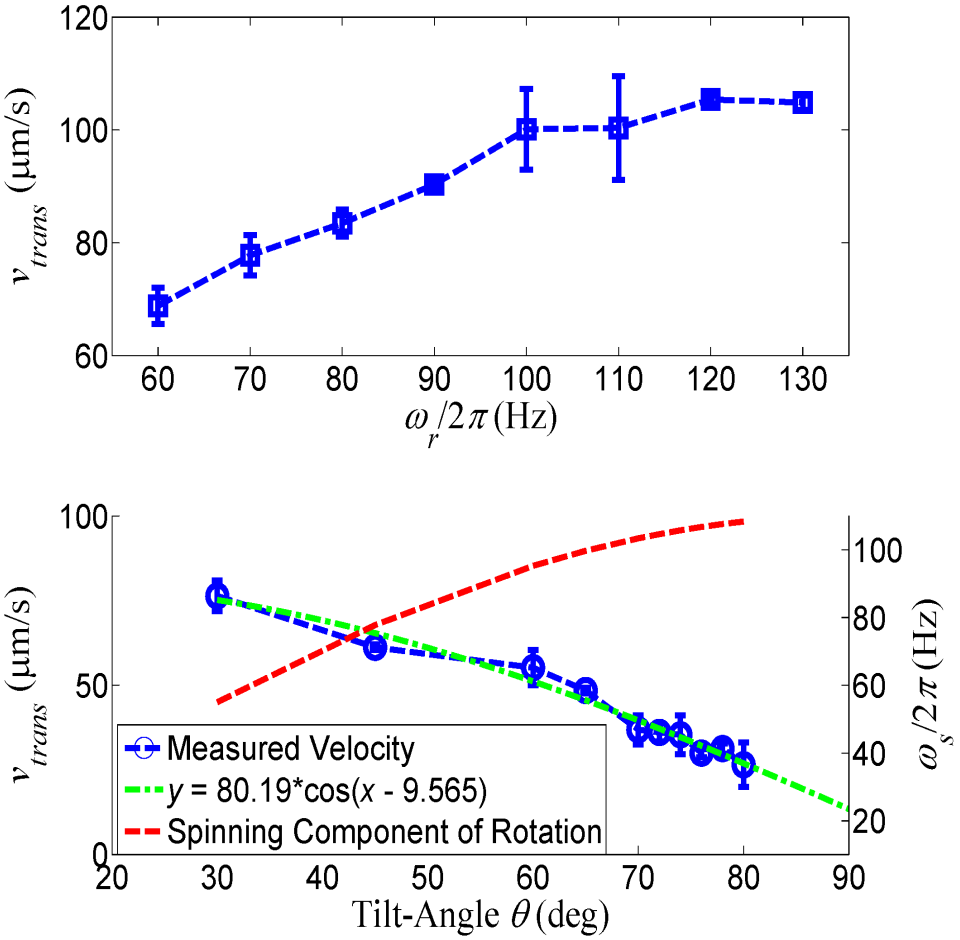

Figure 4

The table of contents entry

Non-contact, selective and dynamic trapping and transportation of motile microorganisms using locally induced flows with minimal damage.